Global and regional health and food security in a Half Earth world

Roslyn Henry (roslynhenry90@gmail.com)
The University of Edinburgh
Almut Arneth
Karlsruhe Institute of Technology
Martin Jung
International Institute for Applied Systems Analysis (IIASA),
Sam Rabin
Karlsruhe Institute of Technology
Mark Rounsevell
Land use change
Piero Visconti
International Institute for Applied Systems Analysis https://orcid.org/0000-0001-6823-2826
Frances Warren
The University of Edinburgh https://orcid.org/0000-0003-0836-547X
Peter Alexander
The University of Edinburgh

Article

Keywords: biodiversity, regional health, food security

Posted Date: April 30th, 2021

DOI: https://doi.org/10.21203/rs.3.rs-415185/v1

Version of Record: A version of this preprint was published at Nature Sustainability on February 3rd, 2022. See the published version at https://doi.org/10.1038/s41893-021-00844-x.

Global and regional health and food security in a Half Earth world.

*Roslyn C Henry[1], Almut Arneth[2,3], Martin Jung[4], Sam S. Rabin[2], Mark D Rounsevell[1,2,3], Piero Visconti[4], Frances Warren[1], Peter Alexander[1,5].

1. School of Geosciences, University of Edinburgh, Drummond Street, Edinburgh EH8 9XP, United Kingdom
2. Karlsruhe Institute of Technology, Institute of Meteorology and Climate Research / Atmospheric Environmental Research, Garmisch-Partenkirchen, Germany
3. Karlsruhe Institute of Technology, Department of Geography & Geo-ecology (IFGG), Karlsruhe, Germany
4. Biodiversity and Natural Resources (BNR) Program, International Institute for Applied Systems Analysis (IIASA), Schlossplatz 1, A-2361 Laxenburg, Austria
5. Global Academy of Agriculture and Food Security, The Royal (Dick) School of Veterinary Studies and The Roslin Institute, University of Edinburgh, Easter Bush Campus, Midlothian, EH25 9RG, United Kingdom

*Corresponding Author: Roslyn C Henry, School of Geosciences, University of Edinburgh, Drummond Street, Edinburgh EH8 9XP, United Kingdom.
Email: roslyn.henry@ed.ac.uk
Telephone: +447835621815

Abstract

Global biodiversity is rapidly declining and goals to halt biodiversity loss, such as the Aichi Biodiversity Targets, have not been achieved. To avoid further biodiversity loss and aid recovery some have argued for the protection of 50% or 30% of the Earth's terrestrial land surface. We use a state of the art global land use model, LandSyMM, to assess global and regional human health and food security outcomes when potential area based strategies for conserving biodiversity are modelled. We find diet and weight changes in strictly enforced 30% and 50% land protection scenarios, cause an additional 5.1 million deaths in 2060. At a regional level, South Asia and Sub-Saharan Africa experience high levels of underweight-related mortality, causing an additional 200,000 deaths in these regions alone. Developed regions in contrast are less affected by protection measures. Our results highlight that radical measures to protect areas of biodiversity value may jeopardise food security and human health in the most vulnerable regions of the world.

Background

The Convention on Biological Diversity committed to halting biodiversity loss [1], however international agreements, such as the Strategic Plan for Biodiversity 2011–2020 and the associated Aichi Biodiversity Targets, have been mostly unachieved. In response to previous shortcomings, ambitious area-based biodiversity conservation measures have been suggested, the proposal to conserve half of the Earth's surface has been the most hotly debated example [2–5]. More recently a 'global deal for nature' target [6], to protect 30% of the earth's surface by 2030, has been adopted by an intergovernmental group of more than 57 countries known as The High Ambition Coalition (HAC) for Nature and People (https://www.hacfornatureandpeople.org/). Whether it is 50% or 30%, area-based targets will form part of post-2020 Global Biodiversity Framework discussions [7]; however, they will need to be scrutinized to ensure their implementation does not compromise other Sustainable Development Goals. In particular, a Half Earth or 30% strategy would require extending protected areas and restoring natural land [2,3,6]. The consequences of this may be felt in food production sectors as agriculture is pushed into smaller areas and marginal land [8]. Reduced food provisioning could potentially compromise food security goals and human health, particularly in vulnerable regions [9]. Given existing food security inequalities, it is important to consider the impacts of conservation measures on human populations in a spatially explicit manner [10].

Scenario analysis has proved to be a powerful tool in identifying measures that are required for effective conservation across different regions [10,11]. Recently, spatially explicit model-based scenarios have been used to explore policies that could reduce threats to conservation from agriculture [12] and to evaluate measures to halt and reverse biodiversity decline while sustaining global food supply [13]. However, most existing scenario approaches have modelled the impact of society and conservation policy on nature [11], while the impact of conservation actions on societies is largely unexplored [8,14,15]. For example, the impacts of widespread area-based conservation measures on food security and health remain poorly understood [9,15]. Furthermore, existing studies of human and biodiversity interactions have been typically conducted at global scales, despite calls to ensure regional variations are considered [11,16].

Here we use a state-of the art modelling framework, LandSyMM [17], to address such gaps. We investigate the human health and food security consequences assuming that stringent and radical conservation measures for biodiversity protection are implemented. We identify priority areas that contribute the most to extinction prevention using an optimization approach and for this study make the assumption that strict protection is established in these areas. We assume that by 2040, 30% and 50% of the earth's terrestrial surface is protected from human use. Results from the protection scenarios are compared with outcomes from a Reference, 'Middle of the Road' Shared Socio-economic Pathways (SSP2) scenario [18,19].

Methods

LandSyMM framework

The Land System Modular Model (LandSyMM)[17], is a state of the art global land use model that couples a dynamic global vegetation model (LPJ-GUESS, SI material) with a food and land system model (PLUM, SI material). LandSyMM generates 'potential yields', using the dynamic vegetation module (LPJ-GUESS), for every grid cell and crop under local climate and soil conditions, and different fertiliser and irrigation regimes while accounting for changing atmospheric CO_2 concentrations and climate. The potential yields are provided to the land use module (PLUM) to project future agricultural areas, fertilizer application, and irrigation intensities to supply agricultural commodities. This land use optimization step is processed at a finer grain in LandSyMM compared to IAMs; most IAMs do their calculations at an economic region level. Furthermore IAMs do not typically consider yields and necessary management under local (e.g. per gridcell) constraints. Country-level demand for commodities is calculated endogenously using an additive demand system rather than being specified exogenously [20,21]. Per-capita income and population levels derived from shared-socioeconomic pathway (SSPs), along with food prices and price elasticities are used to estimate consumption levels. Commodity prices are adjusted in each time step according to global supply and demand. PLUM allows short-term over- and undersupply of commodities relative to demand, therefore relaxing the assumption of market equilibrium.

Scenarios

30% and 50% protection scenarios

The grid cell fractions designated as protected under the 30% and 50% protection scenarios are determined by a spatial conservation prioritisation approach [22]. We use vertebrate distribution data (at ~0.5° resolution) of all birds, mammals, amphibians and reptile species[23,24] . We calculate for each species the amount of area necessary for a species to qualify for a non-threatened status, thus avoiding extinction [22,25]. We then set incremental budgets of available land area (10, 20, 30, 40, and 50% of the global land surface area) and minimize for each species globally the shortfall in reaching those targets, hierarchically locking in proportions of selected grid cells from lower budgets. To account for intraspecific variation and to coarsely represent ecological and genetic diversity of a species, we subdivide each species' range into multiple conservation features using data on the distribution of terrestrial biomes [3]. Further details on the prioritization approach can be found in Jung et al.[22]. All optimizations are solved using the Gurobi optimization software (ver. 8.1)[26] in an integer linear planning approach with the prioritizr package [27]. To create the protection scenarios we here take the priority areas that cover 30% and 50% of the global land surface respectively. For the scope of this work, we assume that the resulting priority areas are stringently protected.

The socio-economic and climate settings for the protection scenarios are the same as those for the Reference scenario, detailed below. However, in the protection scenarios we assume that by 2040 30% and 50% of the terrestrial land surface is stringently protected from agricultural use following the 'nature only' ethos. Between 2020 – 2040 the protection regimes are gradually implemented. In a grid cell with sufficient natural land available to protect, the fraction of natural land requiring protection becomes immediately protected in 2020. However, in grid cells where the fraction of natural land is less than the fraction of protected area required, existing cropland or pasture are gradually removed such that by 2040 the fraction of natural land in a cell is equal to the fraction required to be protected (Figure S2).

Reference scenario

Socioeconomic parameters, population trajectories and GDP trajectories follow the "middle of the road" SSP scenario (SSP2), with trends largely exhibiting historic patterns [28,29]. GDP levels and endogenously calculated food prices drive per-capita demand for food. Under SSP2 GDP continues to increase, driving a shift away from staple crops towards increased consumption of meat, milk, fruit and vegetables (Figure S1). Within SSP2 we assume moderate yield increases of 0.2% per annum due to technological development and management improvement. The climate and atmospheric CO_2 forcing scenario RCP 6.0 is used as it considers the Representative Concentration Pathway [30] most consistent with SSP2 [31]. Forcings are taken from the 1850–2100 IPSL-CM5A-MR outputs from the Fifth Coupled Model Intercomparison Project (CMIP5). While we do not explicitly model bioenergy, demand for bioenergy is important to include as it is an additional pressure on the land system. Demand for first-generation bioenergy is modelled from an observed baseline level in 2010 [32,33] after which it is adjusted to double by 2030 and thereafter remain constant. Global demand for dedicated second-generation bioenergy crops increases to 3263 Mt DM/year by 2060, in line with the SSP2 demand with baseline assumptions [34].

Qualitative changes in parameters were estimated based on an interpretation of the SSP2 storyline [31]. We translate these qualitative estimates of parameters and uncertainty levels into quantitative values characterised by a uniform distribution. A Monte Carlo approach to explore uncertainty associated with input parameters is used and parameters are sampled using a Sobol sequence method with n = 30 over a range of 50% above and below the central parameter values [35]; the central parameter values can be found in Table S1. This approach allows us to capture the uncertainty within the model framework.

Analysis

Food price index

We calculate a Laspeyres food price index (1) in a country *(c)* by calculating how much it would cost the country to meet demand from the base period (year = 2019), for the eight food commodities groups (*f*), in the current period (*t*) given current country specific prices (*p*). The Laspeyres food price index there represents the cost of a basket of goods in a given year compared to the base year.

$$food\ price\ index_{c,t} = \frac{\sum_f demand_{f,c,t=2019} \cdot p_{f,c,t}}{\sum_f demand_{f,c,t=2019} \cdot p_{f,c,t=2019}} \quad (1)$$

Expenditure

We calculate the expenditure on food in relation to GDP to account for GDP changes over time. The expenditure is calculated as the percent of the GDP in a year in a country that is spent meeting demand for food.

$$expenditure_{c,t} = \frac{\sum_f demand_{f,c,t} \cdot p_{f,c,t}}{GDP_{c,t}} * 100 \quad (2)$$

Population weight distributions

We calculate the proportion of the population that is underweight (BMI < 18.5), normal weight (BMI 18.5-25), overweight (BMI 25-30) or obese (BMI 30+) in each country and given year by estimating the mean BMI to use as input in a log normal distribution[36]. We estimate the mean BMI of a country's population using the following relationship:

$$meanBMI_{c,t} = 11.9 + coef_c + kcalPc_{c,t} \cdot 0.0037 + kcalPc_{c,t}^2 \cdot -0.0000002 + percAP_{c,t} \cdot 0.2276 + percAP_{c,t}^2 \cdot -0.0046 + \varepsilon \quad (3)$$

where $coef_c$ is a country fixed effect, *kcalPc* is the average calorie consumption per person per day in a country, *percAP* is the percentage of daily calories consumed in the form of animal products in a country, and ε represents the error term. The relationship in Eq. 3 was estimated by regressing food consumption data from FAOSTAT with WHO estimates of mean BMI for the years 2000 - 2017 (R^2 = 0.87, Figure S3).

We use the estimated mean BMI of a country to calculate the different population weight proportions for a given timestep according to a log normal distribution with a mean:

$$mean_t = Log(meanBMI_{c,t}) - \frac{\sigma_c^2}{2} \quad (4)$$

and standard deviation:

$$sd = \sigma_c^2 \quad (5)$$

Where σ_c^2 is constant over time and calculated by fitting a log-normal distribution to WHO estimates of mean BMI and the prevalence of underweight, overweight and obesity in 2010 using a cross-entropy method. The cross-entropy approach estimates the parameters of the log-normal distribution by comparing two probability distributions and minimising the Kullback-Leibler Divergence.

Deaths avoided

We followed the methodology of Springmann *et al*. [36,37] to calculate the number of deaths avoided in a counterfactual scenario (30% protection, 50% protection) compared to a reference scenario. We isolate the effects of changes in dietary and weight-related risk factors between 2019 and 2060 by comparing the year 2060 in the three scenarios against a baseline with death rates and population structures of 2060 but diets and BMI levels from 2019. We use 2019 as a baseline year as the implementation of 30% and 50% protection begins in 2020. Calculating the mortality differences between the Reference scenario and the protection scenarios in 2060 also allows us to estimate the impacts of the 30% and 50% protection.

We considered deaths caused by coronary heart disease (CHD), stroke (STR), colorectal cancer (CRC), all cancers (TOC), type-II diabetes (DIA) and other causes (OTH) from diet and weight related risk factors. We included three dietary risk factors (fruit, vegetable and red-meat consumption) and four levels of weight-related risks (underweight, normal weight, overweight, obese). The number of

deaths avoided in country (*c*) in year (*t*) for disease (d) according to risk factor (*f*) in age group (*a*) was calculated according to:

$$\Delta deaths_{c,t,d,f,a} = DR_{c,d,a} \cdot P_{c,t,a} \cdot PIF_{c,t,d,f} \quad (6)$$

Where DR is the death rate taken from the Global Burden of Disease Project for the year 2019 [38]. P is the population size of the age group; population size and demographic changes for each country were projected based on SSP2 from the IIASA database [19,39]. The population impact fractions (PIF) are the proportions of mortality that would be avoided if the risk exposure were changed from the Reference scenario to the protection scenarios, while the distribution of other risk factors in the population remain unchanged.

For the dietary risk factors, the PIFs were calculated as follows:

$$PIF_{c,t,d,f} = 1 - \frac{RR_{d,f}^{cm_{c,t,pr}/s_f}}{RR_{d,f}^{cm_{c,t,ref}/s_f}}, \qquad f = (red\ meat\ intake, fruitveg\ intake) \quad (7)$$

where RR is the relative risk of disease/mortality cause for the risk factor. The relative risk factors were taken from Springmann et al.[33] and are given in Table S2. For the dietary risk factors, it was assumed that the whole adult (>= age 20) population of a country experiences the risks associated with its consumption level (*cm*) measured in g/capita/day. We assumed serving sizes (*s*) of 100g [36]. The relative risk is raised to the power of the consumption level over the serving size. Consumption levels are indexed by *pr* and *ref* for their levels in the protection scenarios and Reference scenario, respectively. The commodities included in the dietary risk categories are listed in Table S2.

For the weight related risk factors the PIFs were calculated as follows:

$$PIF_{c,t,d,f} = 1 - \frac{\sum_w P_{c,t,w}^{pr} \cdot RR_{d,w}}{\sum_w P_{c,t,w}^{ref} \cdot RR_{d,w}}, \qquad w = \begin{pmatrix} underweight, normal\ weight, \\ overweight, obese \end{pmatrix} \quad (8)$$

where the relative risks *RR* are differentiated by disease *d* and weight category w. The proportions of the population (*P*) in the different weight categories are differentiated by country and year.

We calculated the combined disease and mortality burden of changes in dietary risk factors and weight risk factors using the following equation:

$$PIFtot_d = 1 - \prod_f \left(1 - PAF_{d,f}\right),\ f = \begin{pmatrix} weight, red\ meat\ intake, \\ fruit\ intake, veg\ intake \end{pmatrix} \quad (9)$$

where PIF_{TOT} is the final PIF for a given disease after all PIFs for risk factors (*f)* have been combined.

Results

Between 2020 and 2040 in the 30% and 50% protection scenarios, biodiversity protection is gradually implemented across the terrestrial land surface such that by 2040, 30% and 50% of the Earth is assumed to be under stringent protection (Figure S2). Such extreme levels of protection and human exclusion have repercussions in the modelled results for food production. Much of the land protected is in temperate and tropical regions (Figure S2); consequently, agricultural land is shifted away from optimal growing areas in these regions and into higher latitudes and marginal land, particularly in the 50% protection scenario (Figure S4). This has the effect of reducing food supply while demand continues to increase with population growth. When demand exceeds supply, food prices increase, which reduces food consumption. This has positive health effects through the reduction of obesity and red meat consumption but negative health effects through increasing levels of undernutrition and reduced fruit and vegetable consumption. Implicitly, reducing levels of obesity reduces the risk of cancer, stroke and coronary heart disease and especially diabetes while reducing red meat consumption is particularly important for reducing the risk of colorectal cancers (Table S2). Conversely, reducing fruit and vegetable consumption increases the risk of cancer, stroke and coronary heart disease while being underweight increases the risk of cancer and death due to other causes (Table S2).

Strict land protection has disparate regional health impacts

	Number of additional deaths (thousands) in 2060 due to changes in diet and weight-related risk factors						
	Total	↓ fruit consumption	↓ vegetable consumption	↑ red meat consumption	↓ underweight	↑ overweight	↑ obesity
Number of additional deaths (thousands) in 2060 due to changes in diet and weight-related risk factors							
Reference	4905	251	1648	2340	-1744	320	1815
30% protection	5122	419	1857	2248	-1657	298	1670
50% protection	5106	549	2041	2043	-1508	261	1426
Number of additional deaths (thousands) in 2060 due to land protection							
30% protection	218	168	209	-93	87	-22	-145
50% protection	201	298	393	-297	236	-59	-389

Table 1: Upper section: Additional global deaths in 2060 in the Reference, 30% and 50% scenarios, using 2019 diets and weight levels as a baseline for comparison. Lower section: Additional global deaths in 2060 due to land protection, calculated as the difference between the number of additional deaths in the Reference scenario and the protection scenarios. Negative values represent fewer deaths. The sum of the individual risk factors for a region can be greater than the total deaths avoided as individual risks can be attenuated and/or compensated when combined with other risk factors.

Compared to 2019, in all three scenarios, there are additional diet and weight related deaths driven by increased levels of obesity, increased red meat consumption and reduced fruit and vegetable

consumption (Table 1, upper section). However, compared to the Reference scenario, the protection scenarios increase global mortality by further reducing fruit and vegetable consumption and maintaining higher levels of underweight related mortality (Table 1, lower section). In the Reference scenario, globally by 2060, there are an additional 4.9 million diet and weight related deaths in 2060 compared to the baseline (Table 1). In 2060 in the 30% protection scenario there are an additional 5.12 million deaths globally, (Table 1) and in the 50% scenario there are an additional 5.11 million deaths globally, (Table 1). Therefore, in 2060, 30% and 50% land protection increases total global mortality by 4%, equivalent to an additional 31 and 28 deaths per million people, respectively (Figure 1). The additional diet and weight related mortality in the protection scenarios are caused by increased food prices relative to the Reference scenario (Figure 3).

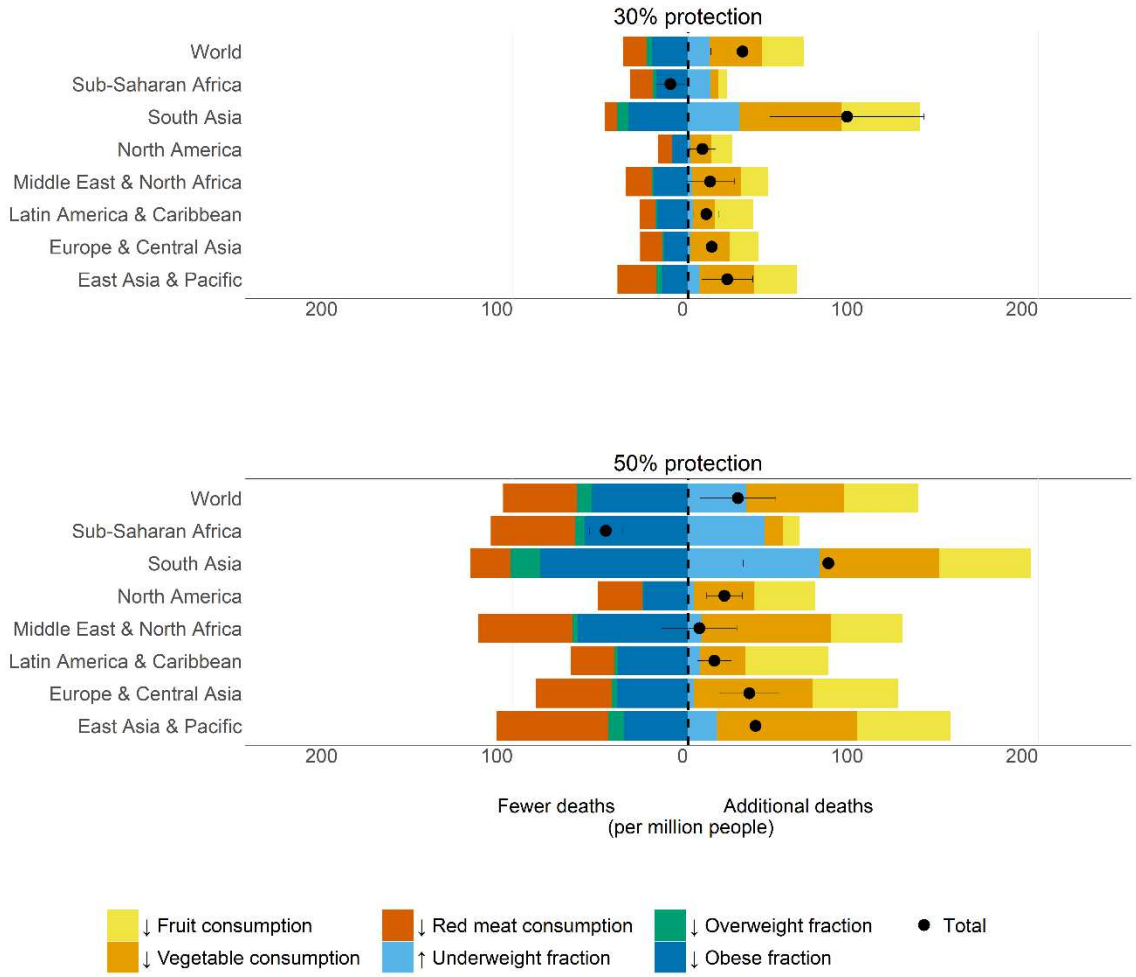

Figure 1: The health effects of protection measures in 2060. The results here show the difference in deaths in 2060 between the (a) 30% and (b) 50% protection scenarios and the Reference scenario. The number of additional and fewer deaths per million people for each world region are shown. Colours represent the different risk factors. Points represent the average total change in deaths, and error bars show the standard deviation (n=30). The sum of the individual risk factors for a region can be greater than the total change in deaths as individual risks can be attenuated and/or compensated when combined with other risk factors.

The protection scenarios reduce fruit, vegetable and red meat consumption compared to the Reference scenario (Table S5, Figure S5, Figure S6). In both scenarios this results in a net increase in mortality, compared to the Reference scenario, from dietary causes (Table 1, lower section). While the net global and regional effects of 30% and 50% protection are similar, changes in dietary risk exposure and associated mortality are much larger in the 50% scenario compared to the 30% scenario (compare width of bars in (a) and (b) of Figure 1). Reduced fruit and vegetable consumption increases deaths globally by 377,000 in the 30% protection scenario and by 691,000 in the 50% protection scenario (Table 1). Reduced red meat consumption reduces global mortality by 93,000 in the 30% protection scenario and by 297,000 in the 50% protection scenario. Therefore in both scenarios the benefits of lower red meat consumption are overwhelmed by the negative consequences of decreased fruit and vegetable consumption.

Likewise, differences in weight risk exposure are much larger in the 50% scenario compared to the 30% scenario. At a global level, the protection scenarios reduce average BMI such that there are 167,000 and 448,000 fewer obesity and overweight related deaths in the 30% and 50% scenarios respectively (Table 1). However, reducing BMI also increases the number of underweight related deaths by 87,000 in the 30% scenario and by 236,000 in the 50% scenario compared to the Reference scenario. Thus, the increase from 30% protection to 50% protection almost triples the additional underweight related mortality in 2060.

There are clear differences in the rate of underweight-related deaths between developing and developed countries. South Asia and Sub-Saharan Africa have the largest additional underweight-related deaths in 2060 compared to the Reference scenario in both the 30% and 50% protection scenarios. In the 50% protection scenario, South Asia and Sub-Saharan Africa have an average of 75 and 44 additional underweight related deaths per million people, equivalent to 196,000 additional deaths in absolute terms (Figure 1, light blue bars). Thus additional underweight related deaths in these regions account for 83% of all global additional underweight related deaths. In contrast, developed regions such as North America and Europe and Central Asia have the lowest additional underweight-related deaths in 2060 compared to the Reference scenario, both with a rate of 3 additional deaths per million people, equivalent to 3717 additional deaths in absolute terms (Figure 1, light blue bars). In 2019, South Asia and Sub-Saharan Africa are the regions with the lowest calorie consumption and subsequently the highest underweight population fractions, 22% and 16% respectively (Table 2). In the Reference scenario by 2060, calorie intake in these regions increases and the underweight population fraction decreases from 22% to 13% in South Asia and from 16% to 7% in Sub-Saharan Africa (Table 2). The protection scenarios stall this decrease, however, and by 2060, the underweight population fraction in the 50% protection scenario is 14% in South Asia and 8% in Sub-Saharan Africa (Table 2). For both regions this is a difference of 1 percentage point between the 50% protection scenario and the Reference scenario (Figure 2).

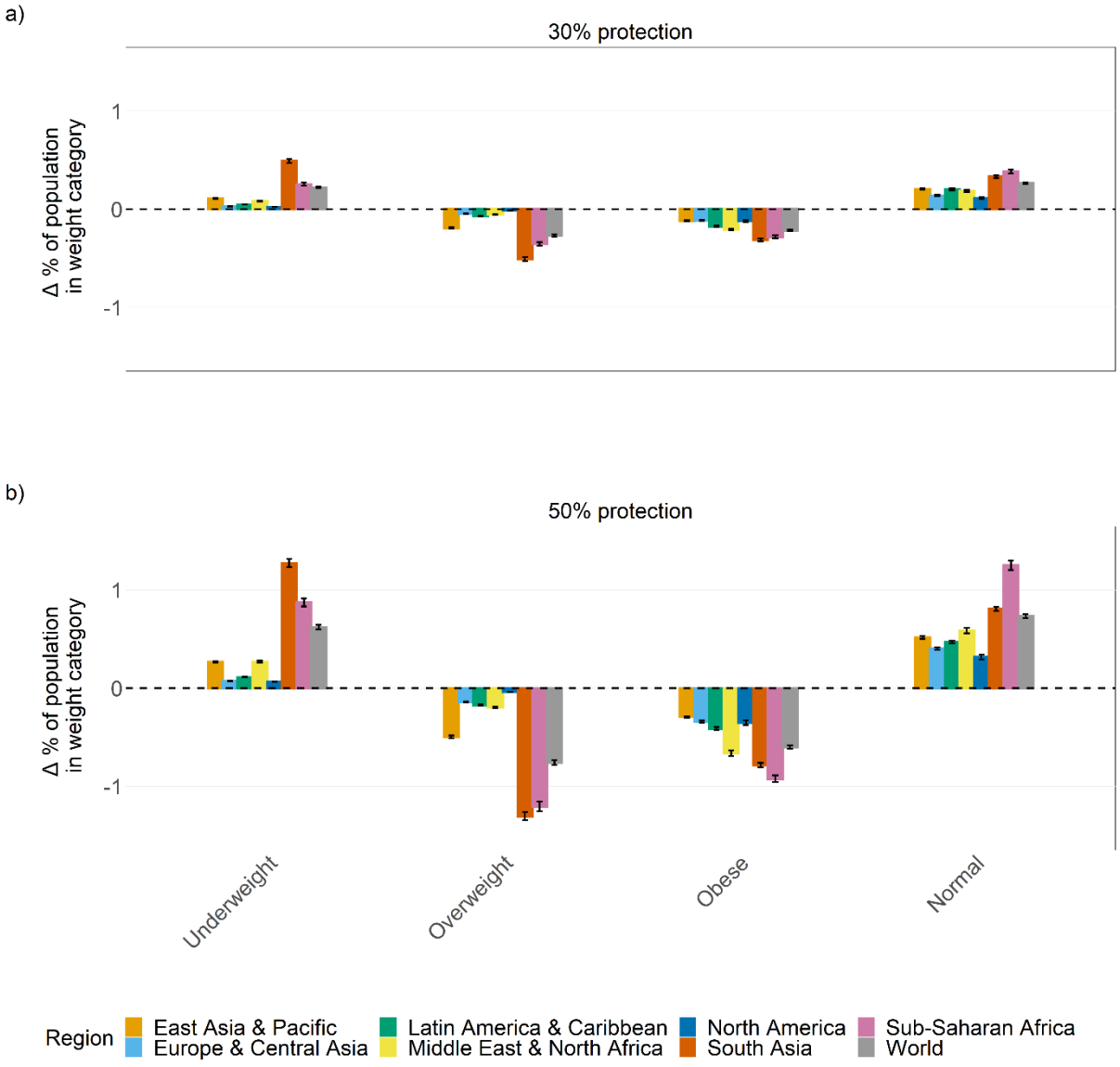

Figure 2: *Difference in the percentage points of each regional population in the four BMI weight categories between the Reference scenario and (a) 30% and (b) 50% protection scenarios in 2060. Y axis values not equal to zero indicate changes as a result of the protection scenarios. Columns represent the mean with standard error bars (n=30). Regional values are a weighted average using country population sizes as the weighting within the region.*

The number of underweight related deaths in South Asia explains why the difference between total mortality in the Reference scenario and the 50% scenario is greatest in South Asia, with 80 additional deaths per million people, more than double the global average. Moreover, the difference in fruit and vegetable consumption between the Reference and 50% protection scenario are greatest in South Asia (Figure S6) and thus mortality due to lower consumption of fruit and vegetables increases relative to the Reference scenario. This combination of additional underweight related deaths and additional deaths due to lower fruit and vegetable consumption acts to increase the net number of additional deaths in South Asia relative to other regions.

Sub-Saharan Africa is the only region where land protection results in fewer deaths compared to the Reference scenario. In the 30% protection scenario, 10 fewer deaths occur per million people and in

the 50% protection scenario, 49 fewer deaths occur per million people. However, while land protection may seem beneficial for Sub-Saharan Africa in terms of net mortality, Sub-Saharan Africa still experiences high numbers of additional underweight related deaths. Unlike other regions, the consumption of fruit and vegetables does not drop substantially in Sub-Saharan Africa compared to the Reference scenario, thus there are fewer deaths related to reduced fruit and vegetable consumption (Figure 1). The difference in fruit and vegetable consumption between the protection scenarios and the Reference scenario in Sub-Saharan Africa is smaller than other regions because of the dynamics in cross-price elasticities in food demand. Sub-Saharan Africa has the lowest income levels and experiences the greatest increase in the price of ruminant products compared to other regions. Consequently, in the protection scenarios, Sub-Saharan Africa experiences the greatest decline in ruminant product consumption compared to the Reference scenario (Figure S6). Plant based foods are substituted for the meat products that are not consumed and, in particular, fruit and vegetables are a common substitute. Therefore, in Sub-Saharan Africa, as land protection reduces the consumption of ruminant products, levels of fruit and vegetable consumption are maintained and as such, the difference in fruit and vegetable consumption between the protection and Reference scenario is smaller for this region.

	Scenario			
	Baseline (2019)	Reference	30% protection	50% protection
East Asia & Pacific				
Underweight	6.63	5.54	5.65	5.81
Overweight	28.92	30.28	30.09	29.79
Obese	6.02	7.35	7.23	7.06
Calories	2916.61	2957.97	2945.06	2925.77
Europe & Central Asia				
Underweight	2.72	2.76	2.79	2.84
Overweight	38.04	37.97	37.92	37.83
Obese	19.80	19.74	19.63	19.40
Calories	3277.06	3264.38	3256.20	3239.51
Latin America & Caribbean				
Underweight	3.98	3.51	3.56	3.63
Overweight	35.75	36.51	36.44	36.34
Obese	17.65	19.15	18.97	18.74
Calories	2943.63	3011.51	2999.48	2983.08
Middle East & North Africa				
Underweight	6.23	4.09	4.17	4.36
Overweight	32.55	34.17	34.11	33.97
Obese	22.08	27.16	26.95	26.50
Calories	3115.34	3110.64	3098.06	3074.99
North America				
Underweight	4.96	5.01	5.03	5.08
Overweight	34.86	34.84	34.83	34.80
Obese	28.16	27.61	27.49	27.26
Calories	3477.36	3442.03	3433.09	3416.20
South Asia				
Underweight	22.02	12.56	13.05	13.84
Overweight	16.52	24.54	24.04	23.24
Obese	3.48	7.36	7.05	6.58
Calories	2567.20	2875.31	2841.52	2801.07
Sub-Saharan Africa				
Underweight	15.57	7.08	7.34	7.96
Overweight	20.97	30.67	30.31	29.46
Obese	5.83	11.62	11.33	10.69
Calories	2555.24	2826.35	2808.33	2774.67
World				
Underweight	10.87	7.15	7.37	7.77
Overweight	26.94	30.63	30.36	29.87
Obese	10.05	12.79	12.57	12.19
Calories	2864.50	2977.03	2958.33	2930.75

Table 2: Global and regional mean weight proportions and daily calorie intake in the baseline year of 2019, Reference scenario in 2060, 30% protection scenario in 2060 and 50% protection scenario in 2060. N=30 and regional averages are calculated by taking a weighted average of the country specific weight levels in a region according to country population size.

Strict land protection increases food prices and spending

Changing dietary consumption levels and weight changes in the protection scenarios are caused by increased food prices relative to the Reference scenario. Furthermore, the greater health impacts in the 50% scenario compared to the 30% scenario are driven by greater food price changes in the 50% protection scenario (Figure 3). Higher food prices in the protection scenarios also increase spending on food relative to the Reference scenario.

During 2020 to 2040, agricultural land is converted back to natural land; this reduces food production, and when demand outstrips supply, food prices increase. In the Reference scenario between 2020 and 2060 food prices decrease due to continued globalisation, climate change and improving production efficiency. With a decline in food prices, the Laspeyres price index falls for all regions (Figure 3). Between 2020 and 2040 in the protection scenarios, the food price index increases, for most regions reaching a peak in 2040. After the implementation period, post 2040, as supply and demand begin to settle and food prices start to stabilise the price index begins to drop, albeit at a slower rate than the rate of increase earlier in the time period (Figure 3). North America, however, continues to experience elevated food prices after 2040 and, in the 50% scenario, the price index stabilises at a value of 2. This is equivalent to a basket of goods costing twice as much as in 2019. The difference in the price index between regions is driven by differences in consumption levels of commodities in the base year of 2019. North America, for example, consumes high levels of ruminant products (Table S5) and therefore the North American price index is particularly sensitive to changes in the price of ruminants. By 2060, the global price of ruminants increases the most relative to other commodities (Figure S7). Thus, because of the greater consumption of ruminants and the greater price increase of ruminants, the North America price index rises substantially. Despite the price index increase, North American expenditure on food remains low (Figure 3), which indicates that developed countries such as the United States of America and Canada are buffered by price increases due to their high GDP.

In contrast, Sub-Saharan Africa experiences the lowest increase in its price index. Consumption of ruminants in Sub-Saharan Africa is among the lowest in 2019, and therefore the large price change in ruminants does not produce as great an increase in the price index for this region. Despite lower food price increases compared to other regions, Sub-Saharan Africa is still vulnerable to even small increases in food prices, as their proportional expenditure on food is the greatest. Indeed, the greatest regional spending difference between the Reference scenario and the protection scenarios is in Sub-Saharan Africa. For example, in Sub-Saharan Africa, by 2060, in the 50% scenario the percent of GDP spent on meeting food demand is 41%, compared to 26% in the Reference scenario. Spending in the protection scenarios increases because global food prices increase between 2020 and 2040 and while GDP increases, it is at a slower rate. After 2040 food prices settle, albeit at higher levels compared to the Reference scenario. This settling of prices causes spending to fall as the rate of GDP increase outstrips any changes in food prices. While by 2060 in all three scenarios spending on food has fallen in most regions, the decline is more pronounced under the Reference scenario (Figure 3); thus, the implementation of 30% and 50% protection increases food spending across world regions.

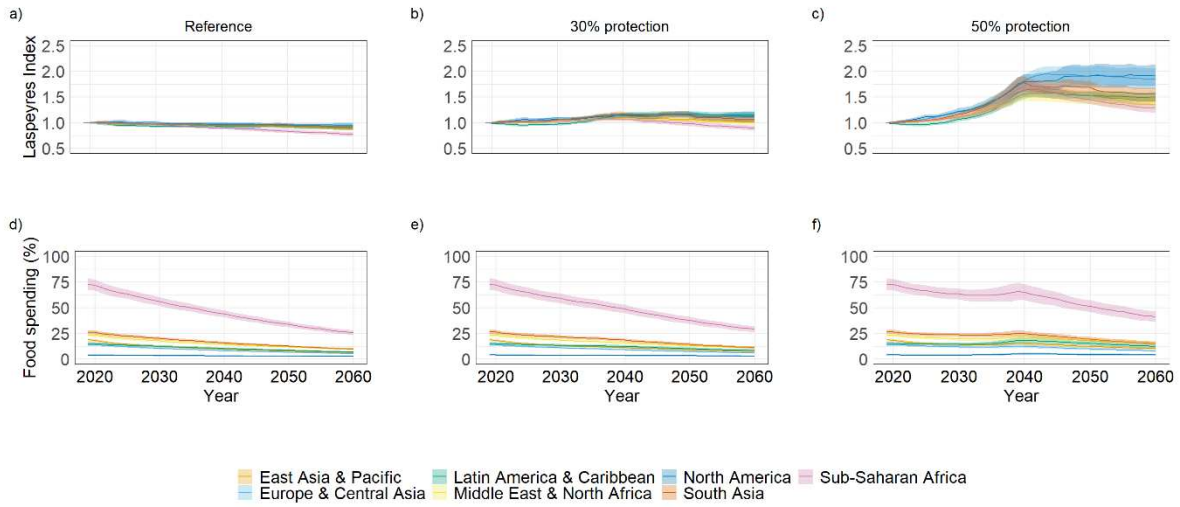

Figure 3: Laspeyres food price index (a,b,c) over time for different world regions in the three scenarios. Food spending as a percent of GDP (d,e,f) over time for different world regions in the three scenarios. The regional index and expenditure are calculated by taking a weighted average of the country specific price index and expenditure in a region according to country population size. The median and standard deviations are shown (n=30).

Discussion

Increasing land protection for biodiversity causes global and regional food prices to increase, which in turn affects food security and human health. Increased food prices reduces calorie intake and the consumption of luxury food commodities, such as red meat, fruit and vegetables. Changing calorie and dietary intake has some positive health effects through the reduction of obesity and red meat consumption related deaths. However, the positive effects are outweighed across almost all world regions by increasing mortality due to increasing underweight population fractions and reduced fruit and vegetable consumption. The 50% land protection scenario results in greater levels of agricultural land resettlement and higher food prices than the 30% protection scenario. Despite this, the additional net global and regional mortality compared to the Reference scenario is similar within the two scenarios, with an additional 5.1 million deaths in 2060 alone.

Considering mortality associated with individual risk factors, rather than net mortality, is however particularly important when considering the trade-offs associated with land protection. When each of the risk factors in our analysis are considered individually, the impact of the 50% scenario is greater than the 30% scenario for all. For example, we find the levels of undernourishment are much greater as the proportion of land protection increases, with the increase from 30% to 50% protection causing an additional 149,000 underweight related deaths and almost tripling underweight related additional mortality in 2060. Similarly, the extent of protection has repercussions for spending. While both protection scenarios slow the reduction of GDP expenditure on food compared to the Reference scenario, all regions experience greater food spending in the 50% protection scenario compared to the 30% protection scenario. Thus, our results serve to

highlight that area-based protection strategies will need to consider the positive and negative repercussions for food security and health for every additional hectare of protection.

We find developed world regions are largely insulated from the negative effects of stringent area-based protection, and arguably reducing calorie consumption and levels of obesity is a desirable outcome; conversely, developing regions are worst affected by reduced food provisioning in terms of undernourishment. Sub-Saharan African countries currently have the highest fraction of undernourishment at a population level while countries in Asia, such as Pakistan and India, are among those with the highest absolute number of undernourished people on the planet [40]. In all of three scenarios, calorie intake increases and underweight related deaths decrease over time. However, land protection lessens the reduction of underweight related deaths, such that in the 50% protection scenario there are an additional 236,000 deaths compared to the Reference scenario, with Sub-Saharan Africa and South Asia accounting for 83% of this additional mortality. In both the 30% and 50% scenarios, underweight related deaths per capita are highest in Sub-Saharan Africa and South Asia. Land protection therefore creates higher levels of undernourishment in regions that are already vulnerable. In a recent modelling study of area based conservation, Kok *et al.* [15] found food security risks as a result of protection measures were most prevalent in Sub-Saharan Africa and South Asia. In our modelled results, we similarly find that Sub-Saharan Africa and South Asia have the greatest proportion of food spending as a percent of GDP in 2019 and the impact of land protection on food spending is greatest in Sub-Saharan Africa. Our results therefore corroborate existing work that finds the food security and health impacts of area-based biodiversity measures are likely to be greatest in some of the most vulnerable societies of the world [8,9,15].

Despite a large number of underweight deaths, land protection results in net fewer deaths in Sub-Saharan Africa. While in our analysis reducing red meat is beneficial for reducing deaths from coronary heart disease, cancer and stroke, it is important to consider that, particularly for regions such as Sub-Saharan Africa and South Asia, access to sufficient protein is often limited. In developed regions such as North America, meat protein can be replaced by other sources because adequate food provisioning is in place. However, for the developing world the benefits from reduced rates of non-communicable disease due to reduced red meat consumption may, in reality, be outweighed by the consequences of lack of sufficient dietary protein if meat is not easily substitutable. We here evaluate the seemingly positive net effect of land protection on Sub-Saharan Africa with scrutiny, given the higher levels of food insecurity and underweight population fractions, and we highlight that future work that includes deaths caused by insufficient substitution of dietary protein may cause additional deaths in developing regions.

For the purpose of this study, we assume that the protection of 30% and 50% of the terrestrial land surface is stringent and food production is excluded from these areas. Our results assume that displaced agricultural land can be reallocated in other regions of the world. Previous modelling efforts have shown that to support conservation without compromising agricultural production, the location of cropland could be optimised [41]. Furthermore, the conversion of agricultural land to natural vegetation, particularly the restoration of forests, could have significant climate co-benefits through increased carbon sequestration [42]. However, while strict protection in area based conservation has been suggested and assessed by some, such as Wilson's original Half Earth proposal [4] and the more recent 'Global Deal for Nature' [3], it is increasingly recognized that conservation management needs to move beyond strict protection [7,43]. Widespread agricultural relocation is unlikely to be feasible or fair and we acknowledge that other forms of conservation management can achieve effective biodiversity protection without complete human and agricultural exclusion. Given contemporary occupation of areas by humans [8], displacement of populations,

particularly indigenous communities, is not a desired outcome. Furthermore in many food insecure regions like Sub-Saharan Africa, agriculture is the main source of income for households, if production is displaced elsewhere there will be further negative impacts related to reduced incomes and economies that we have not captured here. A previous global analysis of a 'nature only' approach to conserving half of every ecoregion found that while it might be possible to achieve such levels of protection, this was at the expense of calorie availability, with a reduction of 25% of crop calories [9]. Similarly a recent modelling approach found a half Earth scenario increased food insecurity in some of the poorest regions of the world [15]. By exploring strict protection, our results serve to further support existing literature, emphasising that the consequences of strict area based protection, particularly comprising 50% of the land surface, would jeopardise global food security and food equality by affecting some of the world's most vulnerable regions.

The results from this work emphasise the need to evaluate human health and food security outcomes associated with area-based conservation, particularly in food insecure regions of the world. Concerning conservation planning, the greatest trade-off to reconcile will likely be with agricultural production [9]. Recently, the Intergovernmental Science-Policy Platform on Biodiversity and Ecosystem Services (IPBES) have developed the Nature Futures Framework (NFF). This framework aims to provide a structure for designing normative scenarios that investigate relationships between humans and nature [10]. In this regard, our results are highly relevant to the IPBES and NFF. Our study is at the extreme end of the spectrum with a nature-only approach and agricultural displacement. Nevertheless, our analysis serves to further highlight that such measures will lead to undesirable and unequal health and food security outcomes. We do not here propose the type of conservation measures that will provide the optimal outcomes for meeting various SDG's, but rather our analysis can provide insight into trade-offs thereby aiding conservation planning and negotiations involving the post-2020 Global Biodiversity Framework.

Acknowledgements

RH, FC, and PA were supported by the UK's Global Food Security Programme project Resilience of the UK food system to Global Shocks (RUGS, BB/N020707/1). MJ and PV acknowledge funding from the Nature Map project through Norway's International Climate and Forest Initiative (NICFI). AA and MR acknowledge support through the Helmholtz Association. SR acknowledges support by the BMBF Germany/ISIPEDIA project.

Declaration of interest

The authors declare no competing interests.

References

1. Butchart, S. H. M. *et al.* Global Biodiversity: Indicators of Recent Declines. *Science (80-.).* **328**, 1164 LP – 1168 (2010).

2. Locke, H. Nature needs half: a necessary and hopeful new agenda for protected areas. *Nat. New South Wales* **58**, 7 (2014).

3. Dinerstein, E. *et al.* An ecoregion-based approach to protecting half the terrestrial realm. *Bioscience* **67**, 534–545 (2017).

4. Wilson, E. O. *Half-earth: our planet's fight for life*. (WW Norton & Company, 2016).

5. Dinerstein, E. *et al.* A "Global Safety Net" to reverse biodiversity loss and stabilize Earth's climate. *Sci. Adv.* **6**, eabb2824 (2020).

6. Dinerstein, E. *et al.* A Global Deal For Nature: Guiding principles, milestones, and targets. *Sci. Adv.* **5**, eaaw2869 (2019).

7. Maxwell, S. L. *et al.* Area-based conservation in the twenty-first century. *Nature* **586**, 217–227 (2020).

8. Schleicher, J. *et al.* Protecting half of the planet could directly affect over one billion people. *Nat. Sustain.* **2**, 1094–1096 (2019).

9. Mehrabi, Z., Ellis, E. C. & Ramankutty, N. The challenge of feeding the world while conserving half the planet. *Nat. Sustain.* **1**, 409–412 (2018).

10. Pereira, L. M. *et al.* Developing multiscale and integrative nature–people scenarios using the Nature Futures Framework. *People Nat.* **2**, 1172–1195 (2020).

11. Rosa, I. M. D. *et al.* Multiscale scenarios for nature futures. *Nat. Ecol. Evol.* **1**, 1416–1419 (2017).

12. Williams, D. R. *et al.* Proactive conservation to prevent habitat losses to agricultural expansion. *Nat. Sustain.* (2020).

13. Leclère, D. *et al.* Bending the curve of terrestrial biodiversity needs an integrated strategy. *Nature* **585**, 551–556 (2020).

14. Visconti, P. *et al.* Projecting global biodiversity indicators under future development scenarios. *Conserv. Lett.* **9**, 5–13 (2016).

15. Kok, M. T. J. *et al.* Assessing ambitious nature conservation strategies within a 2 degree warmer and food-secure world. *bioRxiv* 2020.08.04.236489 (2020).

16. Obermeister, N. Local knowledge, global ambitions: IPBES and the advent of multi-scale models and scenarios. *Sustain. Sci.* **14**, 843–856 (2019).

17. Rabin, S. S. *et al.* Impacts of future agricultural change on ecosystem service indicators. *Earth Syst. Dynam. Discuss.* **2019**, 1–27 (2019).

18. O'Neill, B. C. *et al.* The roads ahead: narratives for shared socioeconomic pathways describing world futures in the 21st century. *Glob. Environ. Chang.* (2015).

19. Riahi, K. *et al.* The Shared Socioeconomic Pathways and their energy, land use, and greenhouse gas emissions implications: An overview. *Glob. Environ. Chang.* **42**, 153–168 (2017).

20. Preckel, P. V, Cranfield, J. A. L. & Hertel, T. W. A modified, implicit, directly additive demand system. *Appl. Econ.* **42**, 143–155 (2010).

21. Gouel, C. & Guimbard, H. Nutrition transition and the structure of global food demand. *Am. J. Agric. Econ.* **101**, 383–403 (2019).

22. Jung, M. *et al.* Areas of global importance for terrestrial biodiversity, carbon, and water. *bioRxiv* (2020).

23. IUCN. The IUCN Red List of Threatened Species. Version 2019.2. 2019

24. Birdlife International. Digital boundaries of Key Biodiversity Areas from the World Database of Key Biodiversity Areas. (2019).

25. Mogg, S., Fastre, C. & Visconti, P. Targeted expansion of Protected Areas to maximise the persistence of terrestrial mammals. *bioRxiv* 608992 (2019).

26. Optimization, G. The State-of-the-Art Mathematical Programming Solver. (2018).

27. Hanson J, Schuster R, Morrell N, Strimas-Mackey M, Watts M, Arcese P, Bennett P, P. H. prioritizr: Systematic Conservation Prioritization in R. (2019).

28. Dellink, R., Chateau, J., Lanzi, E. & Magné, B. Long-term economic growth projections in the Shared Socioeconomic Pathways. *Glob. Environ. Chang.* **42**, 200–214 (2017).

29. Jones, B. & O'Neill, B. C. Spatially explicit global population scenarios consistent with the Shared Socioeconomic Pathways. *Environ. Res. Lett.* **11**, 84003 (2016).

30. van Vuuren, D. P. *et al.* The representative concentration pathways: An overview. *Clim. Change* **109**, 5–31 (2011).

31. Engström, K. *et al.* Assessing uncertainties in global cropland futures using a conditional probabilistic modelling framework. *Earth Syst. Dyn.* **7**, 893–915 (2016).

32. Alexander, P. *et al.* Drivers for global agricultural land use change: The nexus of diet, population, yield and bioenergy. *Glob. Environ. Chang.* **35**, 138–147 (2015).

33. FAOSTAT. Food and Agriculture Organization of the United Nations: Statistics Division. (2016). Available at: http://faostat3.fao.org/. (Accessed: 3rd July 2016)

34. Popp, A. *et al.* Land-use transition for bioenergy and climate stabilization: Model comparison of drivers, impacts and interactions with other land use based mitigation options. *Clim. Change* **123**, 495–509 (2014).

35. Chalaby, Y., Dutang, C., Savicky, P. & Wuertz, D. *Toolbox for Pseudo and Quasi Random Number Generation and RNG Tests Version*. (2015).

36. Springmann, M. *et al.* Health and nutritional aspects of sustainable diet strategies and their association with environmental impacts: a global modelling analysis with country-level detail. *Lancet Planet. Heal.* **2**, e451–e461 (2018).

37. Springmann, M. *et al.* Global and regional health effects of future food production under climate change: a modelling study. *Lancet* **387**, 1937–1946 (2016).

38. Network., G. B. of D. C. Global Burden of Disease Study 2019 (GBD 2019) Results. (2020).

39. KC, S. & Lutz, W. The human core of the shared socioeconomic pathways: Population scenarios by age, sex and level of education for all countries to 2100. *Glob. Environ. Chang.* **42**, 181–192 (2017).

40. FAO, IFAD, UNICEF, WFP, W. *The State of Food Security and Nutrition in the World 2017. Building resilience for peace and food security.* (2017).

41. Tallis, H. M. *et al.* An attainable global vision for conservation and human well-being. *Front. Ecol. Environ.* **16**, 563–570 (2018).

42. Gilroy, J. J. *et al.* Cheap carbon and biodiversity co-benefits from forest regeneration in a hotspot of endemism. *Nat. Clim. Chang.* **4**, 503–507 (2014).

43. Ellis, E. C. & Mehrabi, Z. Half Earth: promises, pitfalls, and prospects of dedicating Half of Earth's land to conservation. *Curr. Opin. Environ. Sustain.* **38**, 22–30 (2019).

44. Alexander, P. *et al.* Adaptation of global land use and management intensity to changes in climate and atmospheric carbon dioxide. *Glob. Chang. Biol.* (2018).

45. UNEP-WCMC., I. &. The World Database on Protected Areas (WDPA). (2019).

46. IIASA/FAO. *Global Agroecological Zones (GAEZ v3.0).* (2010).

SI methods material

LandSyMM modules

PLUM

PLUM is a global land-use and food-system model that combines spatially-explicit, biophysically-derived crop yield with socio-economic scenario data to project future demand, land use, and management inputs[44]. For each country and timestep, the land under cultivation and level of agricultural imports or exports is determined through a least-cost optimisation that meets the demand for food and bioenergy commodities in each country. The demand for food is calculated for eight commodity groups: cereals, oilcrops, pulses, starchy roots, sugar, fruit and vegetables, ruminant products, and monogastric products. Demand is calculated by the modified, implicit, directly additive demand system (MAIDADS)[20,21]. MAIDADS system uses per-capita income levels, food prices and price elasticities to estimate subsistence and discretionary consumption levels and captures the nonlinearity of the relationship between food demand and income. Subsistence and discretionary consumption levels within a country are influenced by income via the utility level, which is indirectly determined by the income level. Discretionary consumption levels respond to price however subsistence consumption is unaffected by price. The demand system gives rise to a relationship between income and food products such that calories are consumed in the form of staple foods (cereals, oilcrops and pulses) at low income levels but this shifts to meat, milk, fruit and vegetables as incomes rise (Figure S1). Conversely, as prices increase, consumption shifts away from 'luxury' goods—such as meat and fruit and vegetables—back towards staple crops. If a country can't afford subsistence levels of consumption then demand for food products is calculated by scaling desired subsistence consumption by the ratio between income available for food expenditure and the desired subsistence consumption.

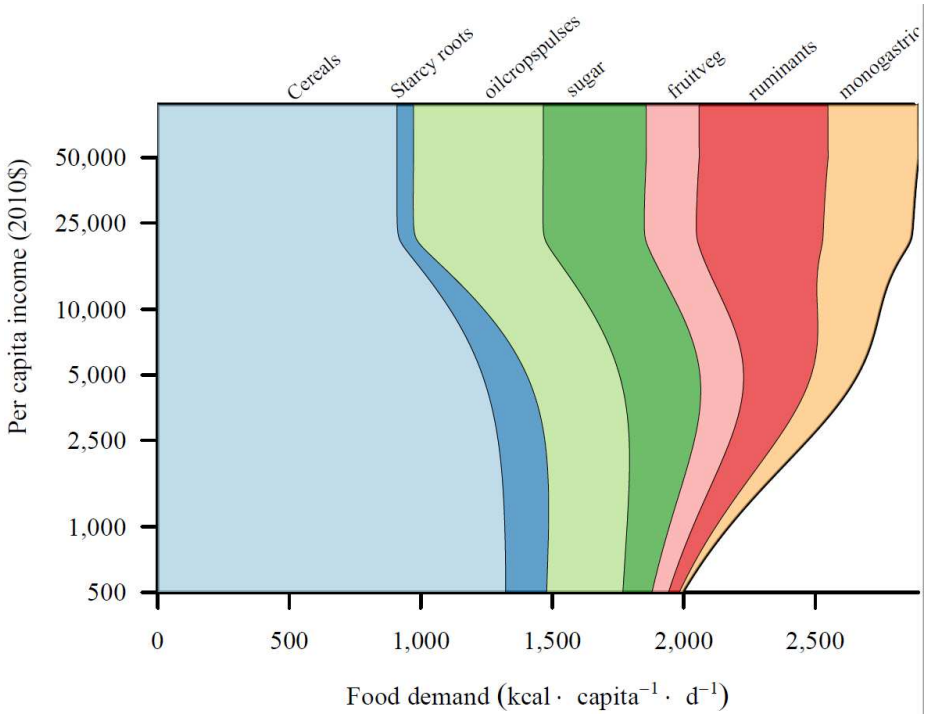

Figure S1: Relationship between per capita income and food demand in PLUM for the seven commodity groups.

Demand for commodities is met by in-country agricultural expansion and/or intensification or from imports from the global market. Commodities produced in excess of a country's domestic demand are exported to the global market. The global market is not constrained to be in equilibrium, instead allowing over- or undersupply of commodities buffered through modelled stocks. Prices are updated for the next year based on global stock levels. For example, oversupply of a commodity on the global market decreases the price as stocks rise, which in return reduces the benefits from its export and reduces the cost of importing it. For each commodity a single tariff free price exists in each time step, which is adjusted for transport costs and other trade barriers, e.g. tariffs, to obtain country specific prices. PLUM determines optimal land-use allocation on a 0.5° grid to meet country level demand. Within the land-use optimisation, PLUM uses spatially specific crop yield responses to intensity inputs, various land-use costs (such as land conversion costs and input costs), protected area constraints and trade costs (see Alexander et al., 2018 for more details on the land-use optimisation).

Land-use optimization also happens at a finer grain in LandSyMM (about 3400 grid cell clusters) than in other similar model systems (tens to hundreds of clusters).

Spatial constraints

The proportion of protected land within a grid cell is calculated using data from the WDPA database[45]. This equates to 1978 Mha or 6.7% of the modelled land surface. Within each grid cell, natural land designated as protected is prevented from conversion to any form of agricultural use; thus, we assume the strictest IUCN classification. In cells where agricultural land already exceeds the area specified as protected, agricultural land is not converted to natural land however no further agricultural expansion can occur. Slope constraints[46] also prevent agricultural use. The slope mask gives the fraction of land allowed for cropland, based on the area in different slope classes from the Harmonized World Soil Database. Cropland is allowed on up to 80% of the second-steepest class (30–45% grade, 27–40.5°) and therefore prevented on steeper slopes which includes land in the steepest class (> 45% grade, 40.5°).

Spatial distribution of protection

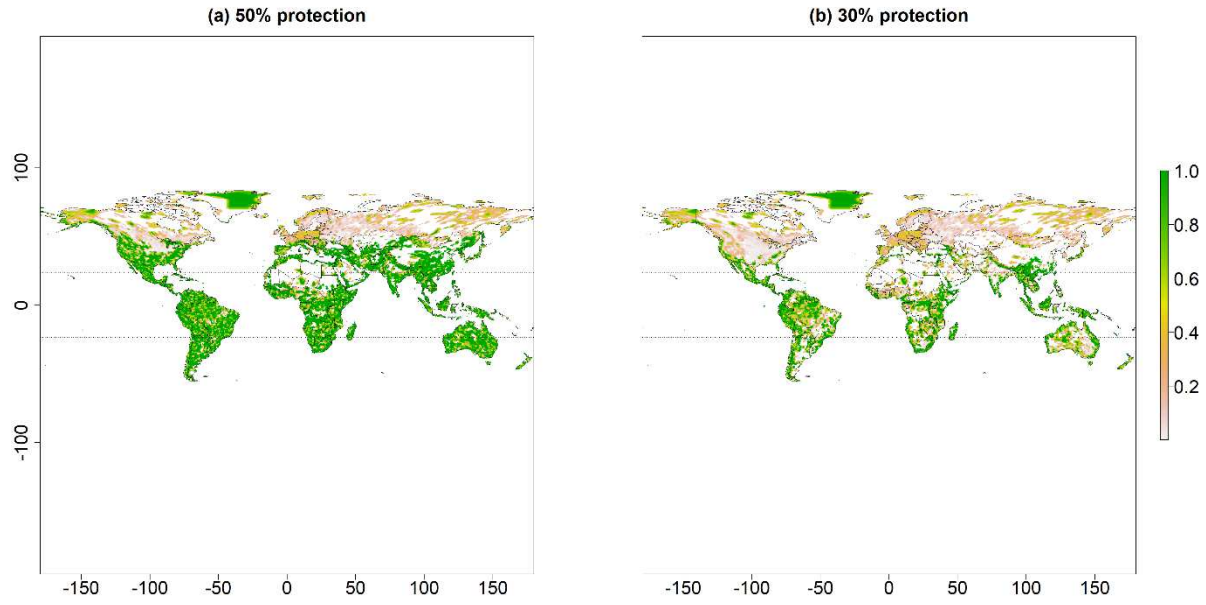

Figure S2: *The proportion of the grid cells protected is shown for the (a) 30% protection scenario and (b) 50% protection scenario. Dotted lines show the subtropical belt (-23.5° to 23.5°).*

Parameter	**Central value**
Irrigation cost, *w_cost* ($/m^2)	0.5
Fertiliser cost, *f_cost* ($/t)	1800
Other intensity cost, *m_cost* ($ at max management input)	600
Land cover change cost, *lc_change*: Natural to agricultural ($/ha)	60
Land cover change cost, *lc_change*: Managed forest to agricultural ($/ha)	160
Land cover change cost, *lc_change*: Agricultural land to natural ($/ha)	200
Land cover change cost, *lc_change*: Pasture to cropland ($/ha)	220
Land cover change cost, *lc_change*: Cropland to pasture ($/ha)	370
Minimum natural or managed forest cover	10%
Pasture harvest fraction	50%
Seed and waste rate	10%
Technology yield change rate, , above that from intensification of production	0.2%
Initial price shift factor	1.0
International market price sensitivity,	0.3
International import tariff, *i_tariff*	20%
Transport costs, *t_cost* ($/t)	50
Transportation losses, *t_loss*	5%
Proportion of animal product substituted by cereals	0.3
Proportion of animal product substituted by pulses	0.35
Proportion of animal product substituted by starchy roots	0.3
Proportion of animal product substituted by oilcrops	0.05

Table S1: *LandSyMM model parameters used. A uniform distribution was sampled across a range 50% either side of the central values.*

Indicators

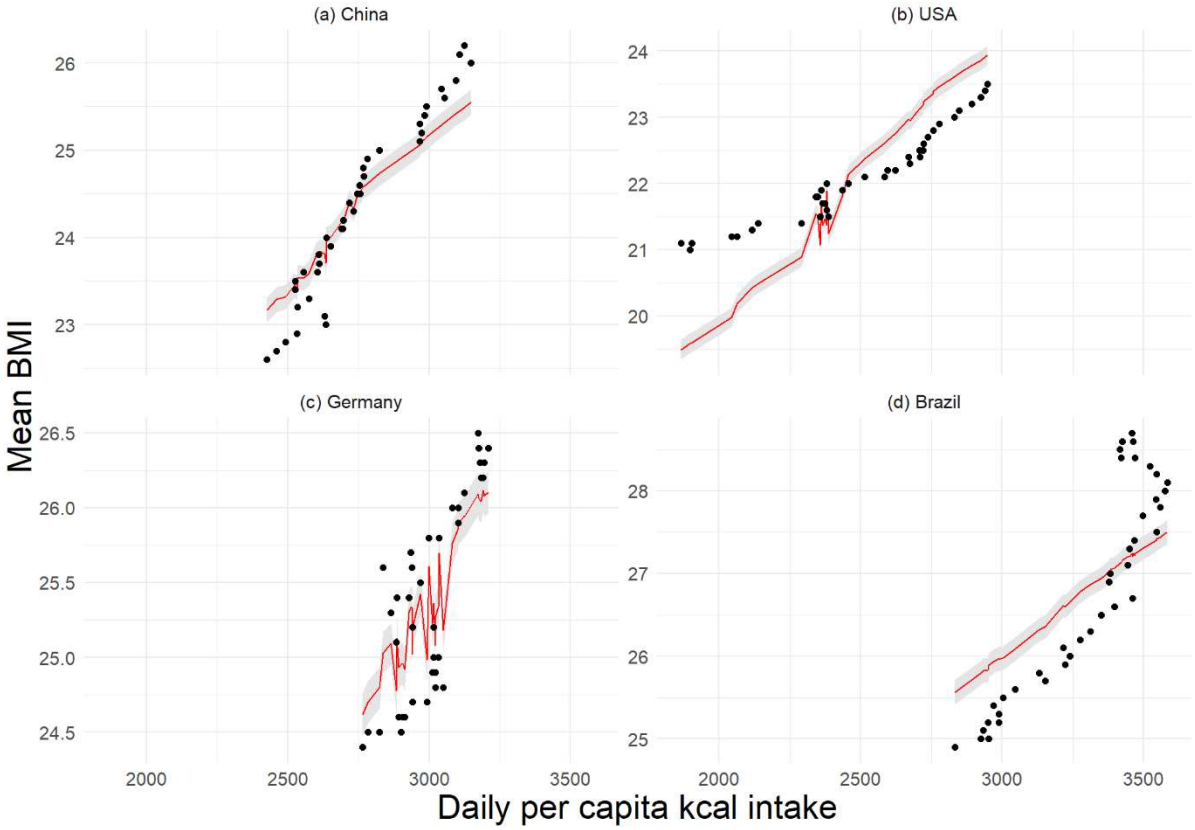

Figure S3: Relationship between daily per person calorie intake and mean BMI based on data from FAO and WHO for the years 2000 – 2017. Data for China, United States of America, Germany and Brazil are shown as examples. The points represent the historic data and the red line represents the fitted model with standard error shown as grey shading.

Risk factor	Relative risk per cause of death					
	Coronary heart disease	Stroke	All cancers	Colorectal cancer	Type-II diabetes	Other causes
Fruit consumption	0.95	0.77	0.94			
Vegetable consumption	0.87	0.95	0.94			
Red meat consumption		1.10		1.15	1.14	
Underweight	0.68	1.03	1.11			1.75
Normal weight						
Overweight	1.31	1.07	1.10		1.54	0.96
Obese	1.78	1.55	1.40		7.37	1.33

Table S2: Relative risk parameters taken from Springmann et al.[36] *supplementary table 9. Blank spaces indicate an absence of evidence to support a relationship between a risk factor and disease endpoint and therefore those pairwise interactions are not included in the analysis.*

Modelled food category	*FAO food category*
Red meat	*Bovine Meat, Meat Other, Mutton & Goat Meat*
Fruit	*Apples, Bananas, Citrus Other, Coconut Oil,Coconuts - Incl Copra, Dates, Fruits Other, Grapefruit,Grapes (excl wine), Lemons, Limes,Oranges, Mandarines, Pineapples*
Vegetables	*Onions, Pepper, Pimento, Plantains, Tomatoes, Vegetables Other*

Table S3: Modelled food categories and FAO commodities included.

Region	Countries
East Asia & Pacific	Australia, Brunei Darussalam, Cambodia, Fiji, Indonesia, Japan, Lao People's Democratic Republic, Malaysia, Mongolia, Myanmar, New Zealand, Philippines, Republic of Korea, Solomon Islands, Vanuatu, Viet Nam
Europe & Central Asia	Albania, Armenia, Austria, Azerbaijan, Belarus, Belgium, Bosnia and Herzegovina, Bulgaria, Croatia, Cyprus, Czechia, Denmark, Estonia, Finland, France, Georgia, Germany, Greece, Hungary, Iceland, Ireland, Italy, Kazakhstan, Kyrgyzstan, Latvia, Lithuania, Luxembourg, Malta, Montenegro, Netherlands, Norway, Poland, Portugal, Republic of Moldova, Romania, Russian Federation, Serbia, Slovakia, Slovenia, Spain, Sweden, Switzerland, Tajikistan, The former Yugoslav Republic of Macedonia, Turkey, Turkmenistan, Ukraine, United Kingdom, Uzbekistan
Latin America & Caribbean	Argentina, Bahamas, Barbados, Belize, Bolivia, Brazil, Chile, Colombia, Costa Rica, Cuba, Dominican Republic, Ecuador, El Salvador, Guatemala, Guyana, Haiti, Honduras, Jamaica, Mexico, Nicaragua, Panama, Paraguay, Peru, Saint Lucia, Vincent and the Grenadines, Suriname, Trinidad and Tobago, Uruguay, Venezuela
Middle East & North Africa	Algeria, Egypt, Iran, Iraq, Israel, Kuwait, Lebanon, Libya, Morocco, Oman, Saudi Arabia, Tunisia, United Arab Emirates, Yemen
North America	Canada, United States of America
South Asia	Afghanistan, Bangladesh, India, Maldives, Nepal, Pakistan, Sri Lanka
Sub-Saharan Africa	Angola, Benin, Botswana, Burkina Faso, Cabo Verde, Cameroon, Central African Republic, Chad, Congo, Cote d'Ivoire Democratic Republic of the Congo, Djibouti, Ethiopia, Gabon, Gambia, Ghana, Guinea, Guinea-Bissau, Kenya, Lesotho, Liberia, Madagascar, Malawi, Mali, Mauritius, Mozambique, Namibia, Niger, Nigeria, Rwanda, Sao Tome and Principe, Senegal, Sierra Leone, Somalia, South Africa, South Sudan, Sudan, Swaziland, Togo, Uganda, United Republic of Tanzania, Zambia, Zimbabwe

Table S4: Regional groupings.

SI results material

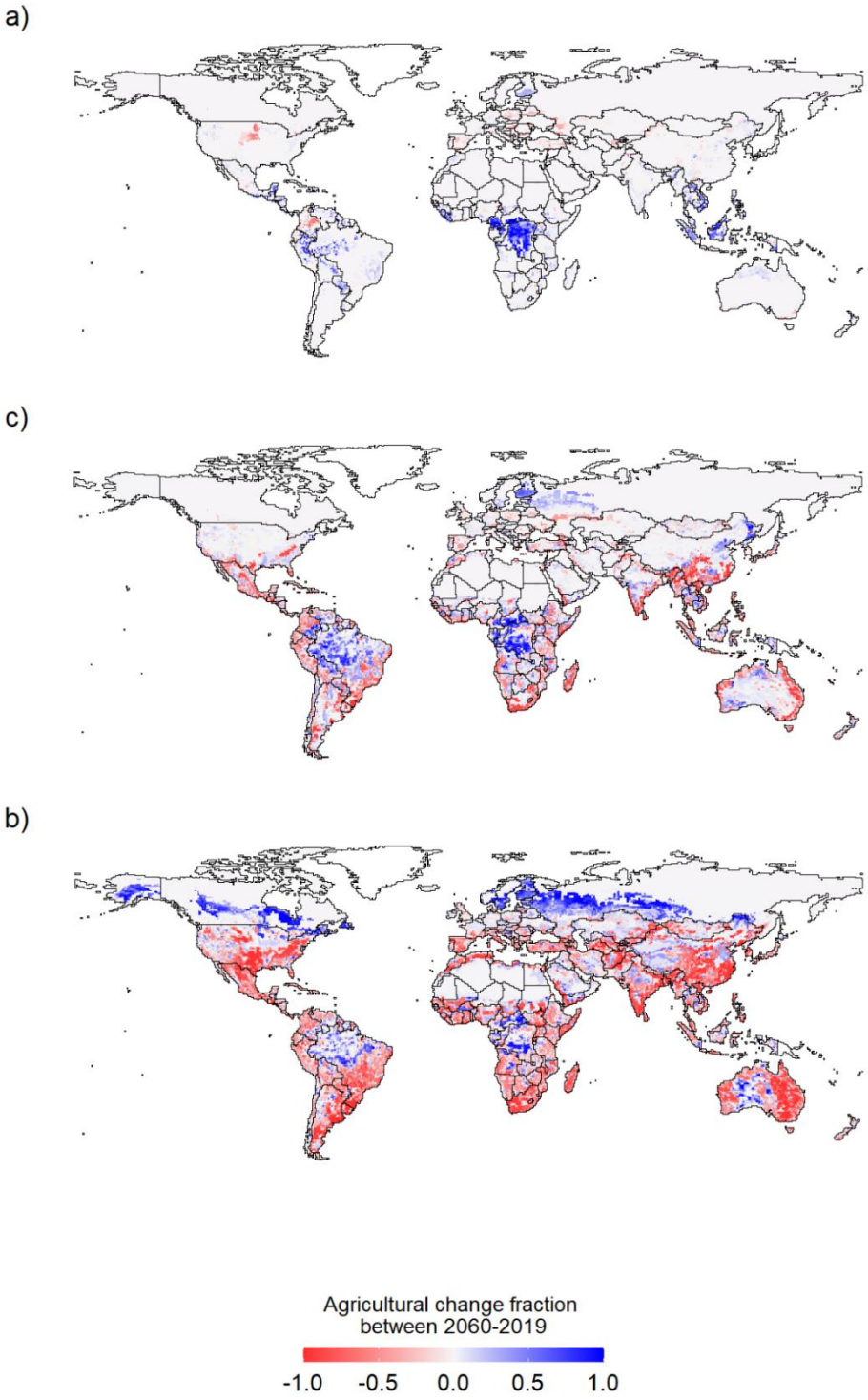

Figure S4: Agricultural land use fraction change between 2019 and 2060 in (a) the Reference scenario (b) the 30% protection scenario (c) the 50% protection scenario. The results of the median parameter run are shown.

	Scenario			
Food type	2019	Reference	30% protection	50% protection
East Asia & Pacific				
Meat	1.202	1.508	1.494	1.469
Fruit	2.404	2.180	2.168	2.153
Veg	6.400	5.168	5.147	5.116
Europe & Central Asia				
Meat	1.404	1.479	1.474	1.460
Fruit	3.115	3.118	3.107	3.085
Veg	3.520	3.489	3.475	3.447
Latin America & Caribbean				
Meat	1.129	1.391	1.383	1.368
Fruit	2.872	2.901	2.873	2.843
Veg	1.835	1.844	1.827	1.807
Middle East & North Africa				
Meat	0.376	0.655	0.647	0.624
Fruit	2.631	2.528	2.513	2.494
Veg	4.451	3.972	3.950	3.916
North America				
Meat	1.760	1.746	1.738	1.721
Fruit	3.210	3.224	3.208	3.179
Veg	3.041	3.048	3.033	3.005
South Asia				
Meat	0.112	0.222	0.215	0.200
Fruit	1.593	1.958	1.897	1.887
Veg	2.133	2.544	2.460	2.446
Sub-Saharan Africa				
Meat	0.370	1.074	1.050	0.981
Fruit	1.257	1.750	1.739	1.728
Veg	1.773	2.447	2.432	2.411

Table S5: Average number of 100g servings of red meat, fruit and vegetables in the seven world regions in the base period of 2019 and in the three scenarios in 2060. N=30.

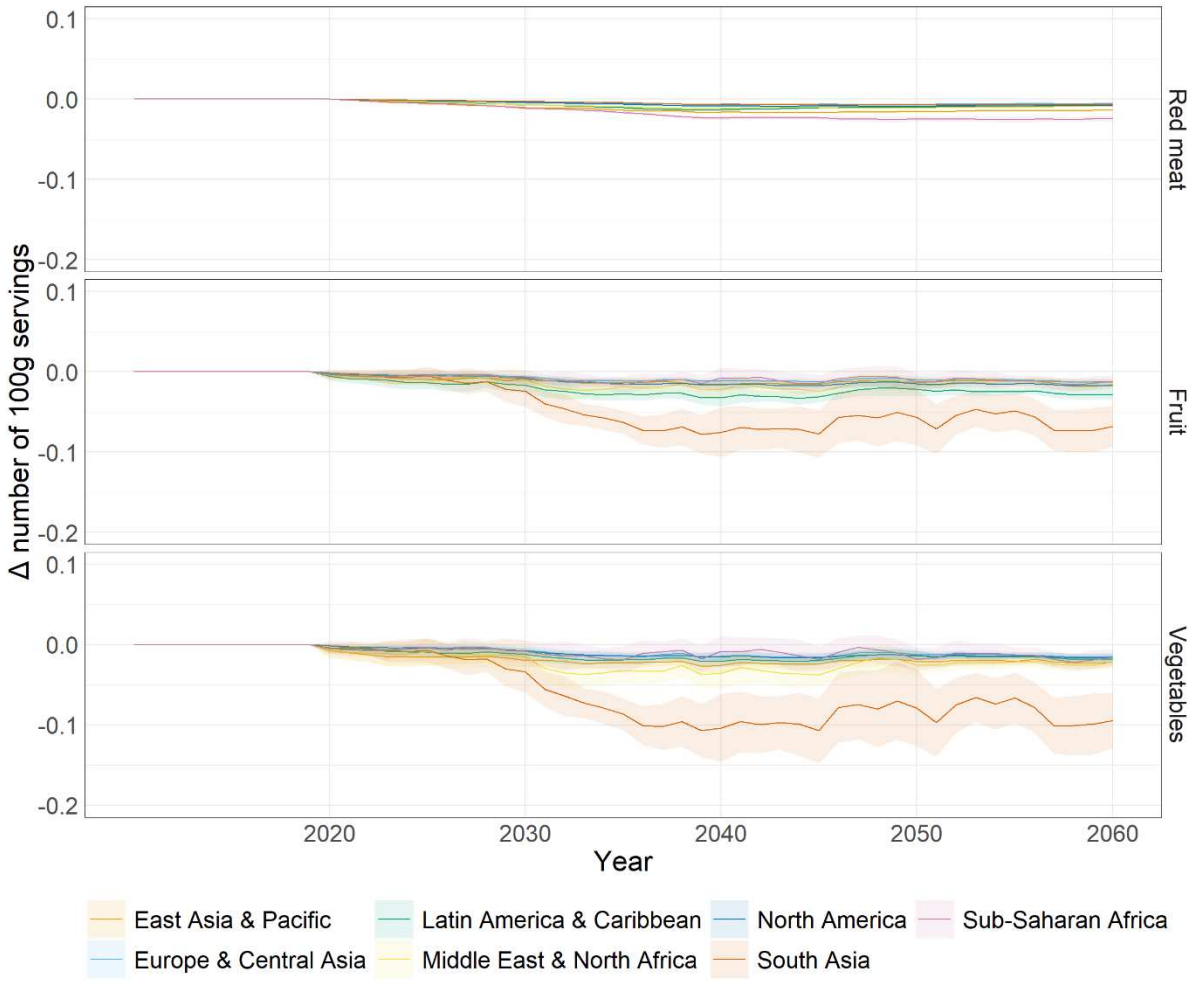

Figure S5: Difference in the number of 100g servings of red meat, fruit and vegetables between the 30% protection scenario and the Reference scenario. Changes in the y-axis value indicate a change as a result of the 30% protection scenario. The median and standard deviation as shown as line and shading respectively. N=30.

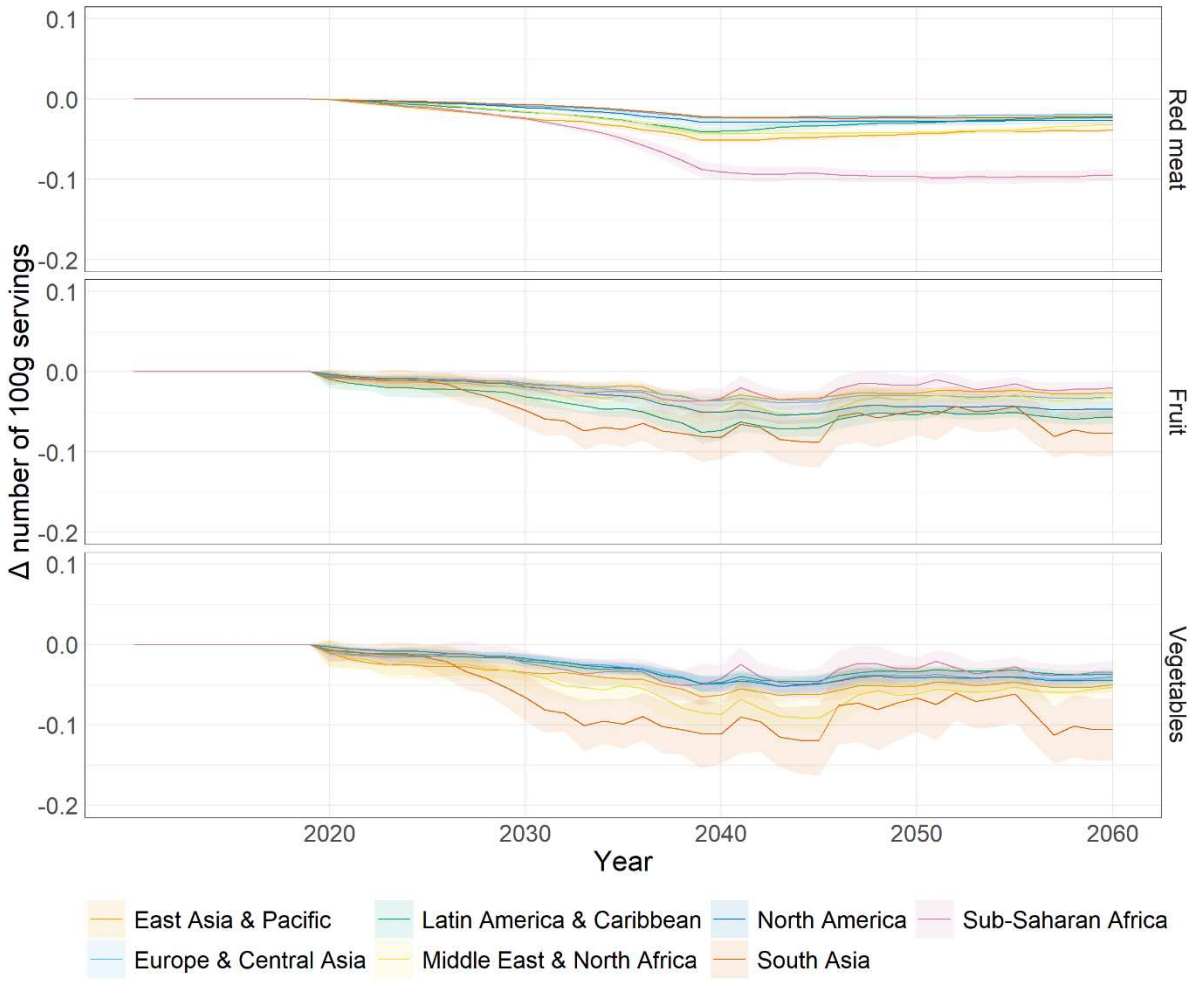

Figure S6: Difference in the number of 100g servings of red meat, fruit and vegetables between the 50% protection scenario and the Reference scenario. Changes in the y-axis value indicate a change as a result of the 50% protection scenario. The median and standard deviation as shown as line and shading respectively. N=30.

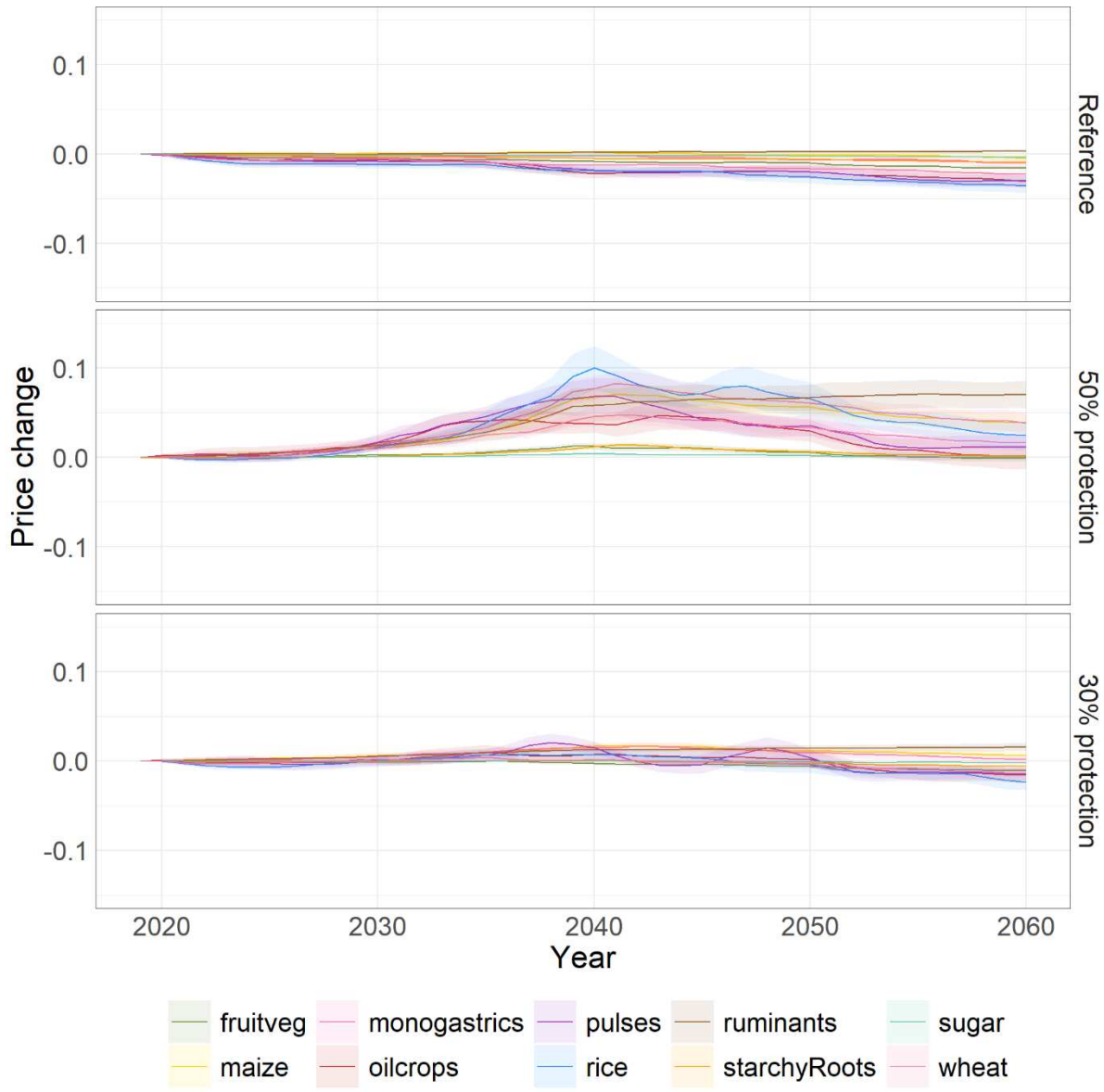

Figure S7: Global price change in the 3 different scenarios for the 8 different commodity types. The median and standard deviation are as shown as line and shading, respectively. N=30.

Figures

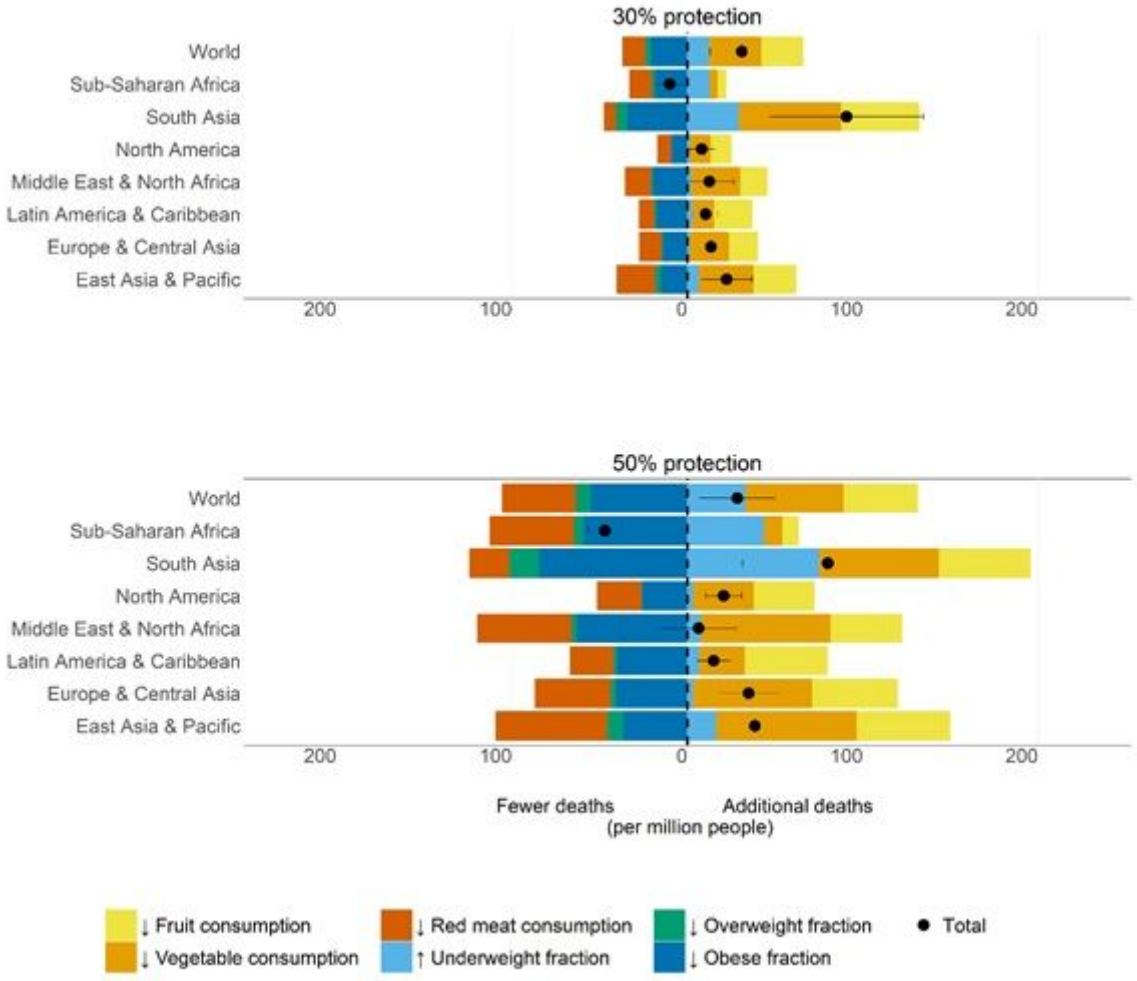

Figure 1

The health effects of protection measures in 2060. The results here show the difference in deaths in 2060 between the (a) 30% and (b) 50% protection scenarios and the Reference scenario. The number of additional and fewer deaths per million people for each world region are shown. Colours represent the different risk factors. Points represent the average total change in deaths, and error bars show the standard deviation (n=30). The sum of the individual risk factors for a region can be greater than the total change in deaths as individual risks can be attenuated and/or compensated when combined with other risk factors.

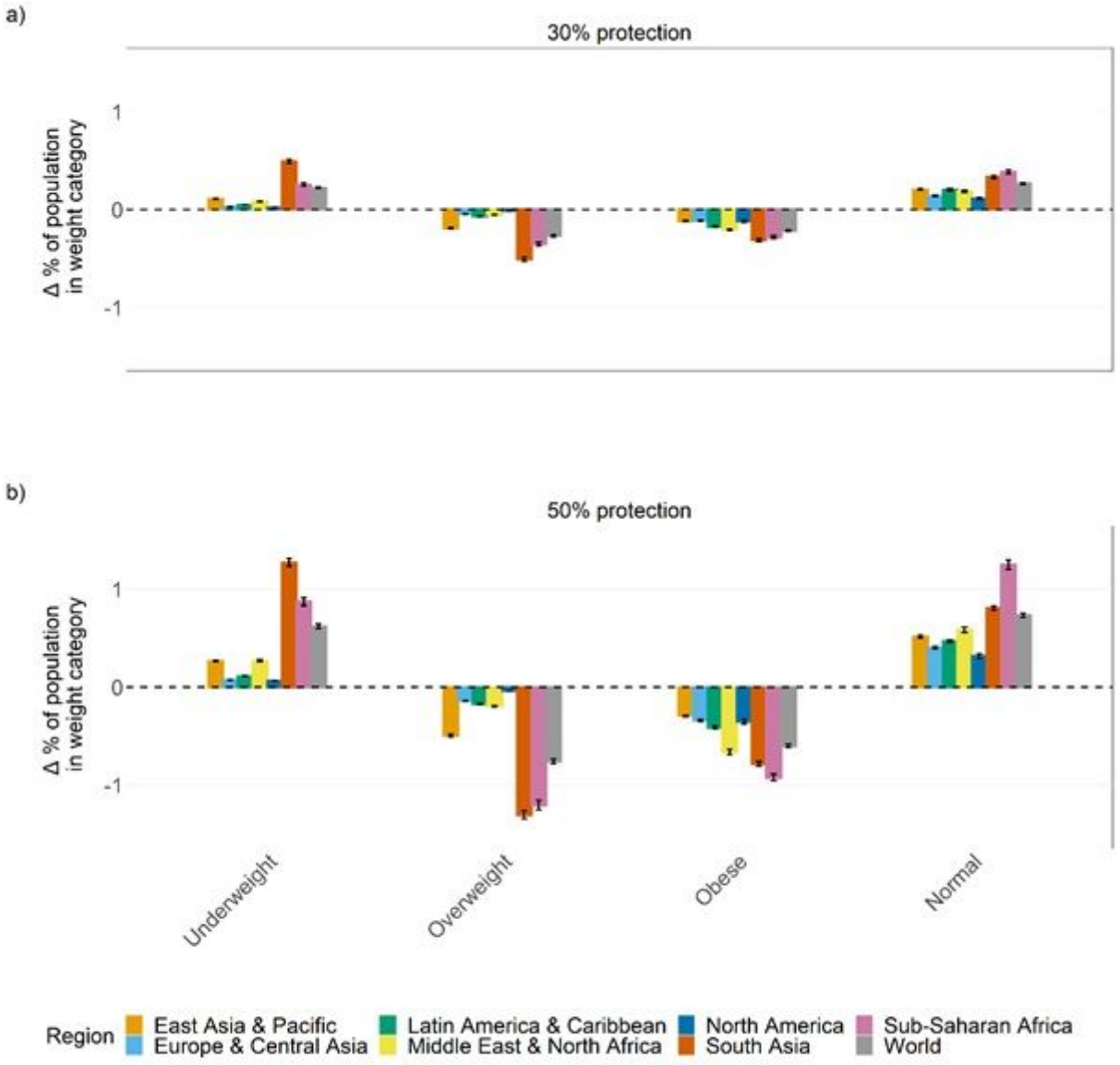

Figure 2

Difference in the percentage points of each regional population in the four BMI weight categories between the Reference scenario and (a) 30% and (b) 50% protection scenarios in 2060. Y axis values not equal to zero indicate changes as a result of the protection scenarios. Columns represent the mean with standard error bars (n=30). Regional values are a weighted average using country population sizes as the weighting within the region.

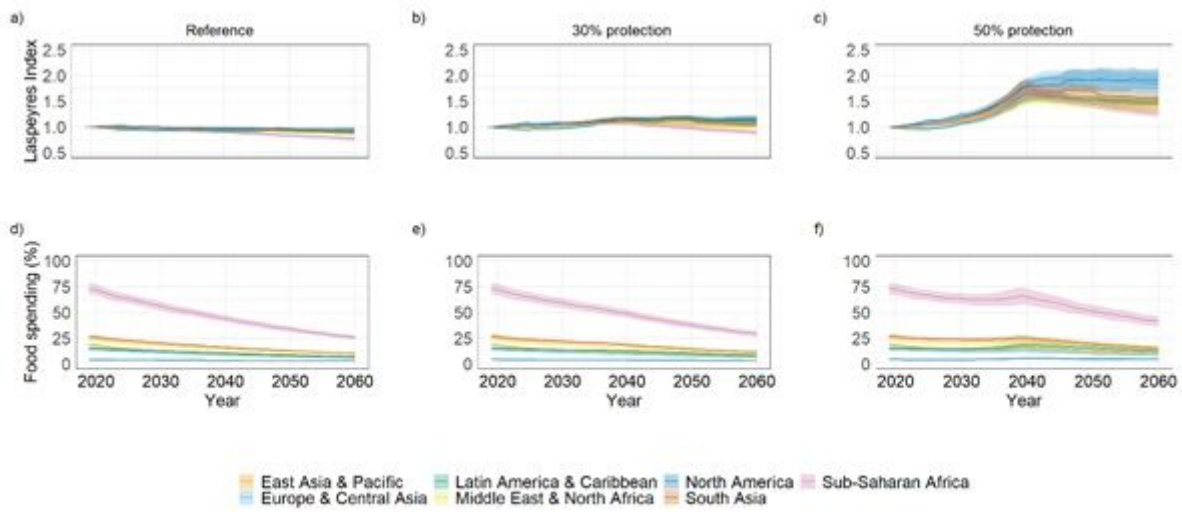

Figure 3

Laspeyres food price index (a,b,c) over time for different world regions in the three scenarios. Food spending as a percent of GDP (d,e,f) over time for different world regions in the three scenarios. The regional index and expenditure are calculated by taking a weighted average of the country specific price index and expenditure in a region according to country population size. The median and standard deviations are shown (n=30).

Supplementary Files

This is a list of supplementary files associated with this preprint. Click to download.

- SImethodsmaterial.pdf